

CONTOURS FROM APPARENT MOTION: A COMPUTATIONAL THEORY

William D. Prophet, Donald D. Hoffman, Carol M. Cicerone

Department of Cognitive Science, University of California, Irvine, 92697 USA

ABSTRACT

Human vision readily constructs subjective contours from displays of kinetic occlusion and color from motion. To construct these contours from kinetic displays it is argued that human vision must solve the point-aperture problem, a problem more general and more difficult than the well-known aperture problem. In the aperture problem one is given a contour and its orthogonal velocity field, and must compute the full velocity field; in the point-aperture problem one is given neither the curve nor any components of its velocity field, and must construct both the curve and its full velocity field. We formalize the point-aperture problem and present, in special cases, two simple algorithms for its solution.

1 INTRODUCTION

In 1911 Pleichart Stumpf introduced the *aperture problem* to explain why rotating spirals appear to expand or contract. The problem, as Stumpf pointed out, is that if one views a moving curve through an aperture sufficiently small that the curve can be well approximated by a line, then only the component of motion perpendicular to the curve can be detected, and other components are lost. Therefore, to obtain a global motion for the curve one must construct one of these other

components, perhaps by combining the locally-detected perpendicular components. The aperture problem is illustrated in Figure 1.

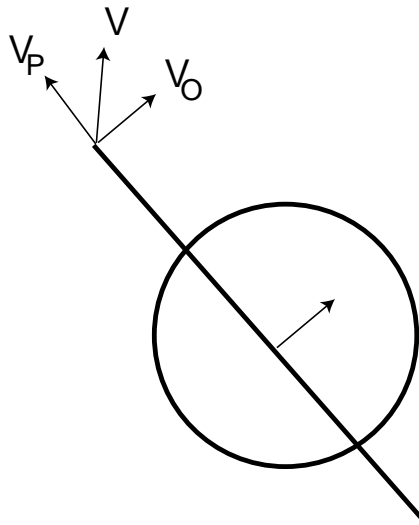


Figure 1. The aperture problem. A small aperture, depicted by the circle, attempts to measure the velocity, V , of a contour passing through it. Due to its limited extent, the aperture can only measure V_O , the component of V orthogonal to the contour. The parallel component, V_P , is invisible to the aperture and must be constructed by later visual processes.

Many researchers have studied the aperture problem with psychophysical experiments (Wallach 1935; 1976; Metzger 1953; Musatti 1975; Scott and Noland 1966; Marr and Ullman 1981; Adelson and Movshon 1982; Hildreth and Koch 1987; Nakayama and Silverman 1988a; 1988b) and with computational theories (Yuille and Grzywacz 1988; Hildreth 1984; Waxman and Wohn 1988; Todorović 1993). The aperture problem assumes that one is given a contour and the orthogonal component of its motion; only one other component of the velocity field along the contour must be constructed. Displays of kinetic occlusion and color from motion (Andersen and Braunstein 1983; Andersen and Cortese 1989; Bruno and Bertamini 1990; Cicerone and Hoffman 1991, 1997; Cicerone et al. 1995; Gibson 1979; Gibson et al. 1969; Kaplan 1969; Kellman and Cohen 1984; Palmer, Kellman, and Shipley 1997; Rock and Halper 1969; Shipley and Kellman, 1993, 1994, 1997; Wallach 1935; Yonas, 1987) often contain no contours, yet human vision readily constructs subjective contours and their motions from these kinetic displays. To do so, human vision must solve what we will refer to as the “point-aperture problem”, a problem more general than the aperture problem. In this paper, we formalize the point-aperture problem and present, in special cases, two simple algorithms for its solution. Our formalization does not address the issue of whether subjective contours seen in static displays arise from the same visual mechanisms as in kinetic displays. Henceforth we will use the term “subjective contour” to be equivalent to the percept of a clearly recognizable contour not present in the physical stimulus.

We begin by describing how to construct displays of color from motion, in which the point-aperture problem arises. The display consists of multiple frames. In each frame a few hundred small colored dots are placed at random on a white background. From frame to frame dots never

change their location, but change their color as follows. Dots within a virtual disk are colored green and all other dots red. In each successive frame the virtual disk is translated a prescribed distance and again only dots within the virtual disk are colored green. The result is a sequence of frames in which the dots do not move, but in which some dots systematically change colors from red to green or from green to red. The first and last frames of a movie created by such frames is shown in Figure 2, with the green dots depicted by the smaller black dots and the red by the larger ones. Within a second or two of viewing this movie, observers see a subjective green disk that glides over the stationary field of dots (Cicerone and Hoffman 1991, 1997). This effect is known as *color from motion*. If the green dots are of higher luminance than the red ones then viewers see a subjective contour surrounding the subjective green disk. By changing the shape of the virtual region (within which color assignments of dots change) to, say, a square, viewers can be made to see subjective borders in the shape of a square with color spreading throughout.

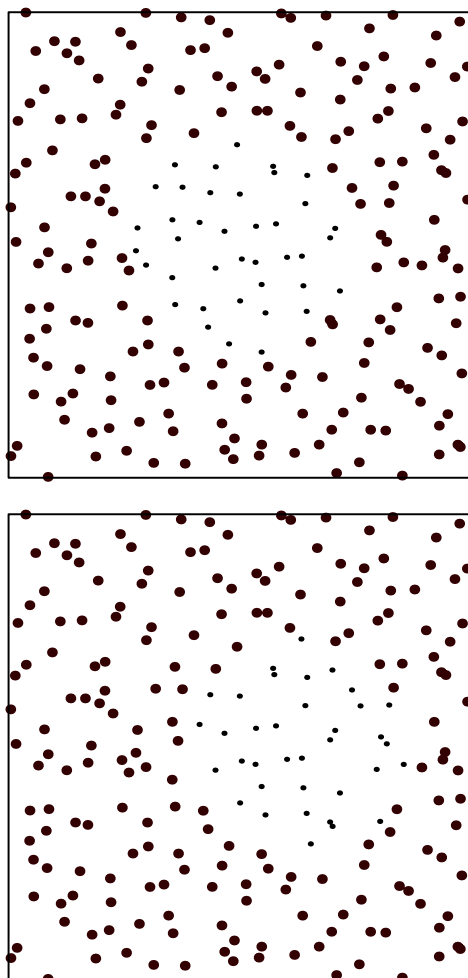


Figure 2. The first and last frames from a display of color from motion that leads observers to perceive a translating subjective disk. No dots change position from frame to frame of the display, but some dots do change color according to an algorithm described in the text.

To construct subjective contours in such displays, observers must solve the point-aperture problem.

Point-aperture Problem: Given a finite set of stationary points and given, as a function of discrete time, which points are to one side of a (virtual) moving contour and which to the other, construct the shape and complete velocity field of the (virtual) contour.

It is helpful to compare this with a succinct statement of the aperture problem.

Aperture Problem: Given a contour and its orthogonal velocity field, construct its complete velocity field.

The aperture problem is a special case of the point-aperture problem. To solve the aperture problem and construct a complete velocity field one need only compute a second component of the velocity field along a given contour. By contrast, to solve the point-aperture problem one must first construct a contour and then compute at least two components of the velocity field along this contour.

In the aperture problem a curve passes through a window so small that only the local differential properties of the curve, viz., the local tangent line and its orthogonal velocity component, can be measured. In the point-aperture problem this window shrinks to a point, precluding the measurement of local differential properties and reducing the available information to one bit: whether the point is to one side of the (virtual) curve or the other at discrete moments in time. This difference is illustrated in Figure 3.

This major difference in what can be measured leads to a corresponding difference in the subsequent constructive tasks. For the aperture problem the constructive task is to compute a total velocity field by integrating the given orthogonal components along the given curve. For the point-aperture problem the constructive task is to compute not only a velocity field but also the curve itself by integrating the bits of information given at discrete points in space and discrete instances in time. Just as there are many ways to solve the aperture problem, there are many ways to solve the point-aperture problem, of which two are described here.

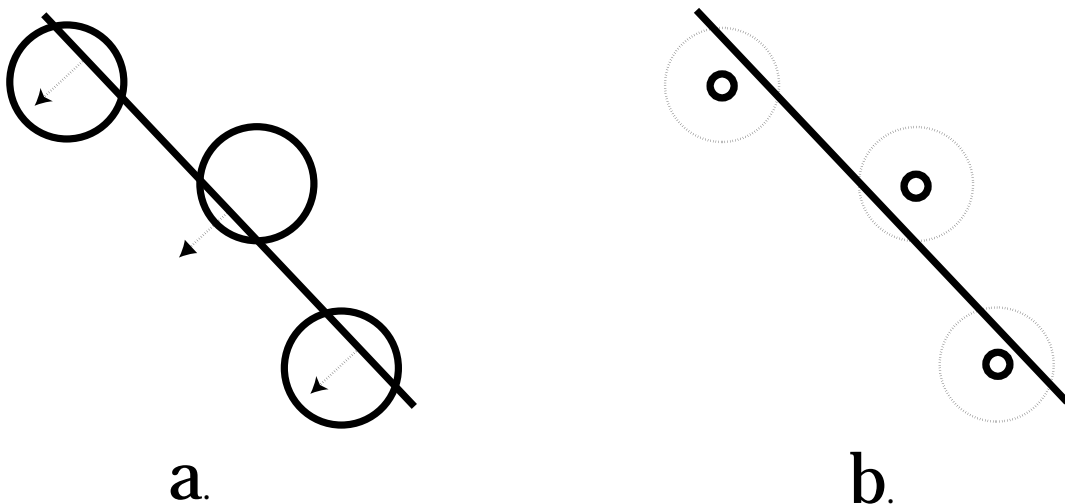


Figure 3. The point-aperture problem compared to the aperture problem. (a) Several apertures measuring the orthogonal velocity of a contour. (b) These apertures now restricted to regions so small that neither the local contour nor its orthogonal velocity can be measured.

2 PHENOMENOLOGICAL MOTIVATIONS

The point-aperture problem, like the aperture problem, is ill posed mathematically: without further constraints one cannot find unique, smoothly varying solutions. A variety of different constraints, leading to a variety of different solutions, can be chosen. In order to obtain a solution which is perceptually plausible, the phenomenology and psychophysics of color-from-motion displays were used as guides for choosing constraints.

Contour Formation Depends on Luminance Contrast

Early work (Liebmann, 1927) showed that the perception of motion is degraded in equiluminant displays. Miyahara and Cicerone (1997) created color-from-motion displays containing regions differing in chromaticity but not in luminance. Viewers still see a spreading of color, but the subjective contour is attenuated. This suggests that the construction of these subjective contours depends primarily on luminance and not on chromaticity information (Miyahara & Cicerone, 1997).

Variable Distinctness

As mentioned above, we see subjective contours in color-from-motion displays with randomly-placed dots. In such displays the density of dots is typically not uniform but varies from one region to another. The clarity of the subjective contour varies with this density: the contour is strongest in regions of high density and weakest in regions of low density. Therefore, the construction of a segment of subjective contour depends primarily on the image data in the neighborhood of that segment (Andersen & Cortese, 1989; Shipley & Kellman, 1993).

Spatial Smoothness

The subjective contour is typically smooth and has no inflections that are not suggested by the data points. Therefore, in the construction of subjective contours, human vision seems to employ a constraint of spatial smoothness (Shipley & Kellman, 1994). This is similar to a constraint like Grimson's "no news is good news": we create no "complications" in the contour without explicit evidence demanding the complication (Grimson, 1981).

Isolated Spatial Discontinuities

The subjective contours that we see in displays of color from motion can have sharp corners. We can, for example, see a subjective square with four sharp corners. A smoothness constraint would never, of course, construct sharp corners. This indicates that a corner-producing process, antagonistic to the smoothness constraint, must also be at work in our construction of subjective contours. Algorithms

have been studied for some time that incorporate both a smoothness constraint and a process that creates corners (e.g., Weiss, 1990), although the issue is still unresolved.

Concave Segments

The convex hull (Hocking and Young, 1961) has proved useful in many vision algorithms. However, it is easy to create displays of color from motion in which viewers see a subjective contour that has clear concavities. For example it is easy to create displays in which viewers see a subjective contour in the shape of a banana. This suggests that human vision does not construct subjective contours by an algorithm requiring a convex hull. A more general approach to the construction of subjective contours is needed.

Temporal Smoothness of Shape

In displays of color from motion, the dots never move, only color assignments of individual dots change. Nonetheless, a subjective contour is seen to move over these static dots. Although the arrangement of dots within the subjective contour changes radically from frame to frame, as illustrated in Figure 2, the subjective contour does not change shape, unless the dot density becomes too sparse to support contour formation. For instance, in some displays of color from motion, viewers see a disk of unchanging shape moving over the field of dots. This suggests that human vision may tend to minimize the variation in time of the shape of the subjective contour (Shipley & Kellmann, 1997).

Temporal Smoothness of Motion

In displays of color from motion, viewers often see the motion of the subjective contour as smooth. However, as mentioned above, there is no motion of dots in these displays, rather only changes in dot colors. This suggests that, in constructing the motion of the subjective contour, human vision uses a constraint of smoothness of motion.

Isolated Motion Discontinuities

It is easy to create displays of color from motion in which viewers see a subjective contour move in a particular direction with uniform velocity, and then suddenly change direction, before once again moving with uniform velocity. This indicates that smoothness of motion is not the only constraint being used in human vision. If we think of the visual system as trying to minimize some functional in its construction of the motion of these subjective contours, then we can think of this functional as having two penalty terms. One term penalizes smooth portions of the motion for high variations in acceleration, a second term penalizes isolated points of motion discontinuity. Abrupt changes

of direction are seen in those circumstances in which there is less penalty for inserting a motion discontinuity than for constructing a smooth motion with high variation in acceleration.

Nested Curves

Displays can easily be created in which observers see an annulus with both an outer and inner subjective contour. This demonstrates that the visual processes which construct these subjective contours are sophisticated enough that they can construct several contours at once (Cunningham, Shipley, & Kellman, 1998).

Tolerance for Color Inhomogeneity in the Test Region

In the displays of color from motion discussed so far, all dots on the “inside” have been one color, say green, and all dots on the “outside” have been another color, say red. Displays in which the chromaticities of test dots are assigned probabilistically can also be created (Cicerone & Hoffman, 1997). Each dot inside the virtual disk has a higher probability of being green but some probability of being red, while each dot outside has a higher probability of being red, but some probability of being green. Over a range of probabilities in such displays, viewers can still see a subjective contour despite a high degree of color inhomogeneity. This suggests that, to handle this color inhomogeneity, there may be a process prior to the point-aperture problem in which the visual system uses spatial or temporal windows to compute statistics to determine “inside” versus “outside” decisions for each dot. For example, green dots outside the filter may be consistent with a background of multicolored dots, against which a green object or filter must be detected.

Volumetric Interpretations

It is possible to create a color-from-motion display in which one perceives a boundary not just in two dimensions, but in three. If the motion of a rotating virtual ellipsoid is simulated, and the dots inside its virtual occluding contour are colored differently from those outside, a dynamic color spreading over the surface of a three-dimensional ellipsoid will be seen, and the boundary contour will appear to be the occluding contour of this ellipsoid (Cortese and Andersen, 1991, first showed this in the achromatic case; Cicerone and Hoffman, 1991, in the chromatic case). This indicates that human vision can solve the point-aperture problem by constructing subjective contours in three dimensions.

Partial Invariance

The perceived shape of the subjective contour does not, in general, change if the entire color-from-motion display is translated. Similarly we find that the perceived shape is scale and rotation invariant as others have with similar stimuli (e.g., Shipley & Kellman, 1993). This suggests that human vision

respects these invariances in constructing subjective contours.

3 FORMALIZATION

In this section we formalize the point-aperture problem.

Point-Aperture Problem: Given a set $P = \{p_1, \dots, p_n\}$, $p_i \in \mathbb{R}^2$, and given at each time $t \in \{1, \dots, m\}$ a copy P_t of P partitioned into subsets I_t and O_t , construct for each t a piecewise smooth plane curve α_t that *divides* I_t and O_t , and construct a velocity field V_t on α_t .

The set P represents the dots in a color-from-motion display. Each copy P_t is called a “frame” of the display. The sets I_t and O_t are called, respectively, the dots “inside” (of higher luminance) and “outside” (of lower luminance). A curve α_t *divides* I_t and O_t if any plane curve joining any $p_i \in I_t$ with any $p_j \in O_t$ crosses α_t .

The point-aperture problem is ill-posed: At each time t there are infinitely many curves α_t which divide I_t and O_t . Therefore we need further constraints.

One constraint mentioned in the last section is temporal smoothness: When subjects view displays of color from motion, they report that the curves α_t appear to deform smoothly rather than arbitrarily, by deformations that are small or zero. This suggests the following approach: stack the frames P_t evenly in sequence, in effect making the time coordinate t a depth coordinate. Then construct a *surface*, S , surrounding the points I_t . The curves $\alpha_1, \dots, \alpha_m$ are obtained as intersections of S with the sequence of planes $t = 1, \dots, m$. The velocity fields V_1, \dots, V_m are obtained by computing appropriate partial derivatives on S .

Thus the point-aperture problem is solved by constructing a single surface. Given this formulation, an extensive literature on surface construction can be immediately applied (e.g., Blake 1989; Szeliski 1990; Weiss 1990).

The construction process, whether of a sequence of curves or of a single surface, depends most critically on those dots that change luminosity from one frame to the next. These are dots that have just been crossed by the boundary defining the luminosity change, so they provide maximal information about its location. They are therefore called “border dots”.

At each time t , $1 < t \leq m$, the border dots B_t are those dots in I_t that were not in I_{t-1} together with those dots in I_{t-1} that were not in I_t . That is, B_t is the symmetric difference of I_t and I_{t-1} ,

$$B_t = I_t \triangle I_{t-1} = (I_t - I_{t-1}) \cup (I_{t-1} - I_t).$$

As can be seen, B_t is the union of two sets. The first, $I_t - I_{t-1}$, contains the dots accreted at time t ; this set we label A_t . The second, $I_{t-1} - I_t$, contains the dots deleted at time t ; this set we label D_t . Thus the border dots B_t can be written as the union of the accreted and deleted dots at time t .

$$B_t = A_t \cup D_t.$$

These two sets play different roles in the process of constructing a curve or surface: the deleted dots must be just outside the constructed curve or surface, whereas the accreted dots must be just inside it.

In the next sections we present two different methods for solving the point aperture problem: the back-projection and border-surface algorithms. Both algorithms generate a set of border dots that must then be used to construct a curve or surface which passes near these dots. The back projection method is for the special case of a rigid object undergoing translation without rotation, and the border-surface method works in the more general case that allows deformation.

4 RIGID TRANSLATIONS: THE BACK-PROJECTION METHOD

In this section we solve the point-aperture problem for the special case of a rigid object undergoing uniform translation without rotation. The color-from-motion display first described in the introduction, in which a disk is seen to move over a field of dots, is an example of such a case. Another example is kinetic occlusion, also described earlier. For kinetic occlusion the border dots at time t are those points accreted or deleted at time t .

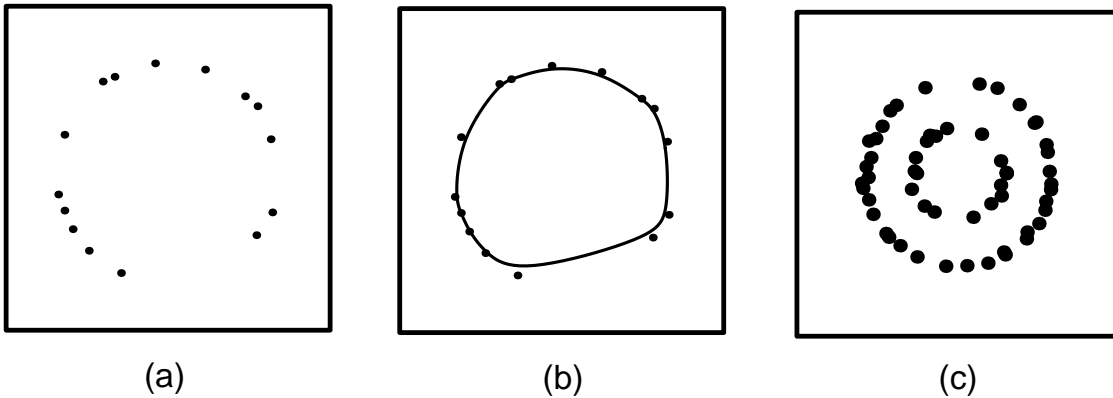


Figure 4. Border frames determined by the back-projection algorithm. (a) The border frame determined from 10 frames of a color-from-motion display depicting a moving disk. The first and last frames of the display are shown in Figure 2. (b) The curve α , constructed as a sequence of cubic spline curves that pass near these border points. Human vision almost certainly uses a more sophisticated approach than cubic splines. (c) The border frame determined from 5 frames of a color-from-motion display depicting a moving annulus.

A simple algorithm for this case is the “back-projection method” defined as follows: Given a sequence of partitioned frames P_1, \dots, P_m with inside dots I_1, \dots, I_m , let the coordinates of each dot $p_i \in P$ be $p_i = (x_i, y_i)$. Compute the mean translational velocity, T , of the inside regions by subtracting the center of mass of I_1 from that of I_m and dividing by m .

$$T = \left(\frac{\sum_{p_j \in I_m} x_j, \sum_{p_j \in I_m} y_j}{m|I_m|} \right) - \left(\frac{\sum_{p_j \in I_1} x_j, \sum_{p_j \in I_1} y_j}{m|I_1|} \right),$$

where $|A|$ is the size of set A . For each set of border dots, B_k , create a translated set of dots \tilde{B}_k , by translating back each border dot $p_i \in B_k$ by the vector $-(k-1)T$. Then create a “border frame”, B , by taking the union of these \tilde{B}_k :

$$B = \bigcup_k \tilde{B}_k.$$

Construct a (piecewise) smooth curve, α , based on the dots in B , by using say the spring interpolation method of Weiss (1990). The velocity field along α is T . The value of the functional that is minimized to obtain α represents the strength of the percept of the contour α .

The back-projection algorithm for determining the border frame B was implemented and run in Monte Carlo simulations.

In the first example the back-projection algorithm was given seven frames of a color-from-motion display in which is seen a disk undergoing uniform translation along the x axis. The first and last frames of this display are shown in Figure 2. The border frame determined by the algorithm is shown in Figure 4a. As can be seen in this figure, the points of the border frame fit nicely around a circle of the appropriate radius. Thus this border frame provides a good data set for interpolating a boundary curve, as shown in Figure 4b. If the color-from-motion display is altered so that an annulus is seen rather than a disk, then one obtains nested border frames, as shown in Figure 4c.

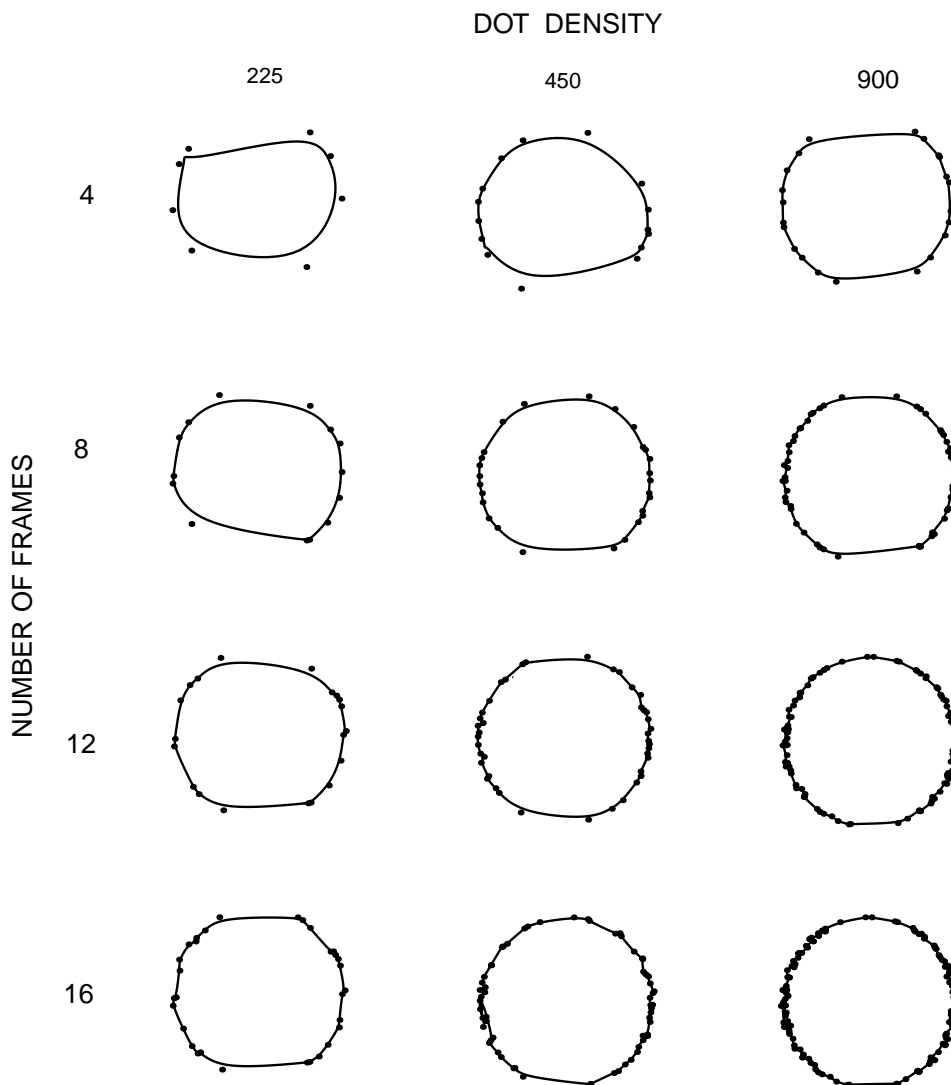


Figure 5. Border dots and interpolating cubic splines for three levels of dot density and four levels of frames. Derived from a display of color from motion that depicts a translating disk. Not represented in this figure is the perceptual strength of the interpolated contours.

With fewer frames, or fewer dots per frame, the border set can become sparse. In this case the back-projection algorithm predicts that one will perceive a well-defined boundary only in those regions for which there are adequate border dots. This is illustrated in Figure 5, which shows the border dots and interpolating cubic splines (Foley and van Dam, 1982) for three levels of dot density and four levels of frames. This fits with the observation noted earlier that the illusory boundary seen in a color-from-motion display can appear better defined in some regions than in others.

In the second example the algorithm used seven frames of a color-from-motion display in which is seen a square undergoing uniform translation along the line $y = x$. The first frame of this display is shown in Figure 6a, with the green dots depicted as smaller than the black ones. The border frame determined by the algorithm is shown in Figure 6b. As can be seen in this figure, the points of the border frame fit reasonably close to a square of the appropriate size. Thus this border frame also provides a good data set for interpolating a boundary curve.

The Monte Carlo trials were based on color-from-motion displays depicting a disk undergoing uniform translation. Figure 2 shows frames typical of these displays. Seventeen hundred displays were generated at random (points chosen according to a uniform distribution), with the number of dots in each display varying from 16 to 400. Each display consisted of four frames in which the disk translated 4.17% of its radius per frame.

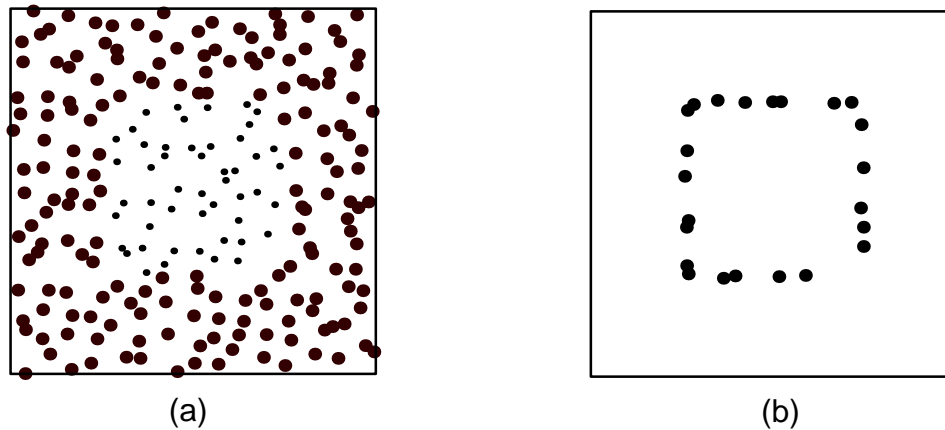


Figure 6. The back-projection algorithm applied to a square. (a) One frame from a color-from-motion display depicting a moving square. (b) The border frame determined by the back-projection algorithm using 10 frames of this display.

The results are summarized in Figure 7. Figure 7a plots the mean number of border dots per frame (vertical axis) as a function of the mean number of dots that were within the disk. As expected, the number of border dots per frame increases as the total number of dots within the disk increases. Figure 7b plots the mean distance of border dots from the origin computed by the algorithm, again as a function of the mean number of dots that were within the disk. The distribution of values obtained by the algorithm approximates the actual value 0.24. As the mean number of dots within the disk increases, the algorithm's estimate of the disk's translation velocity becomes more stable, leading to a more accurate computation of the border frame. As can be seen in Figure 7c, the variance of

the distribution decreases with increasing dot density.

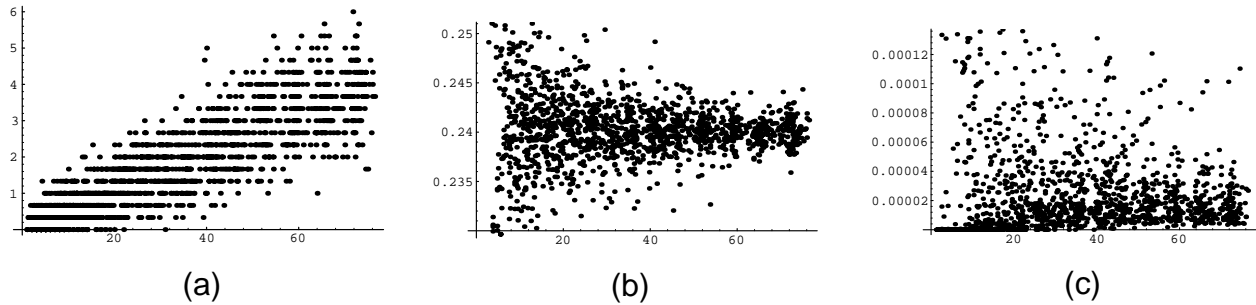


Figure 7. Monte Carlo test of the back-projection algorithm. The results are shown for 1700 displays depicting moving disks. (a) Mean number of border dots per frame, plotted as a function of mean number of dots within the disk. (b) Mean distance of border dots from the origin, plotted as a function of mean number of dots within the disk. The correct value was 0.24. (c) The variance in distance of border dots from the origin, plotted as a function of mean number of dots within the disk.

Thus, the back-projection method is an effective algorithm to solve the point-aperture problem for kinetic occlusion and for color-from-motion displays depicting rigid bodies that translate but do not rotate.

5 TRANSLATIONS AND DEFORMATIONS: THE BORDER SURFACE METHOD

The back-projection method of the last section cannot handle the more general case in which a color-from-motion display represents an object that deforms or rotates as it translates. A border frame does not work in this more general case, because its construction depends on the assumption that α does not deform as it translates.

In this case the “border dots” can be constructed as follows. As before, a sequence of partitioned frames P_1, \dots, P_m with inside dots I_1, \dots, I_m are given, and the coordinates of each dot $p_i \in P$ can be represented by $p_i = (x_i, y_i)$. To each dot in border set B_t , $1 < t \leq m$, an appropriate depth coordinate is attached, giving the “embedded border set”

$$B'_t = \bigcup_{p_j \in B_t} (x_j, y_j, ct),$$

where $c \in \mathbb{R}^+$ is a scale factor for converting time into a depth dimension. The embedded border sets are stacked to create the final “border dots”

$$B = \bigcup_{t=2}^m B'_t.$$

A piecewise-smooth surface, S , is constructed using B as the data points, with a method such as that of Weiss (1990) or Blake (1989). The intersection of S with the plane $z = t$ gives the boundary

curve at time t , viz., α_t . The boundary α_t will in general deform as t varies, and its center of mass will translate. The velocity field, T , along α_t is given by the time derivative

$$T(s) = \left. \frac{dS}{dt} \right|_{\alpha_t(s)},$$

where s is a natural parameter, such as arc length, along α_t .

An example of this method is shown in Figure 8. Part (a) shows the first and last frames of a display in which a disk appears to expand as it translates to the right (green dots are depicted as larger than the black dots). Part (b) shows a stereo view of the border dots computed by the border-surface method. As expected, these dots appear to lie on the surface of a truncated cone. The conical surface which can be seen in this figure demonstrates that the border dots can be a sufficiently rich data set to support the interpolation of the proper surface.

6 DISCUSSION

We have seen that displays of kinetic occlusion and color from motion raise an interesting computational problem for the visual system, a problem we have called the **point-aperture problem**:

Given a finite set of stationary points and given, as a function of discrete time, which points are to one side of a moving contour and which to the other, construct the shape and complete velocity field of the contour.

We have argued that this problem is more general than the aperture problem, because neither the contour nor its orthogonal velocity field are given. Human vision solves this problem nonetheless.

We have presented two algorithms for solving the point-aperture problem. The back-projection algorithm assumes that the contour translates rigidly at constant velocity and does not rotate. This algorithm uses the green test dots—used to recover the object of interest—to estimate the center of mass of this object and to track it over frames. Using the center of mass seems a plausible way that human vision might work. The results of our simulations with this model (shown in Figures 4–6) indicate some interesting psychophysical predictions, namely that (1) as dot density decreases, subjective borders should become less clear perceptually; (2) as dot density increases, sharp corners should be more visible; (3) as dot density decreases, motion from frame to frame should appear less smooth; and (4) in principle, any rigid, nonrotating shape should be perceivable.

The border-surface method goes one step beyond the back-projection method by allowing contours to deform, rotate, and translate nonuniformly. Although this method applies more generally than the back-projection method, it is not an algorithmic generalization. In particular it does not use a center of mass, because for objects that can rotate and change scale the center of mass cannot help to compute an interpolating contour: reverse translations of the center of mass do not lead to a consistent set of border points for interpolation. Rather than a two-dimensional contour interpolation, this method works in a three-dimensional space-time framework to interpolate a surface by tagging sets of border dots with a time coordinate represented as depth. This algorithm makes all the same psychophysical predictions as the back-projection method, but in addition predicts that nonrigid and

rotating shapes can be perceived (Figure 8).

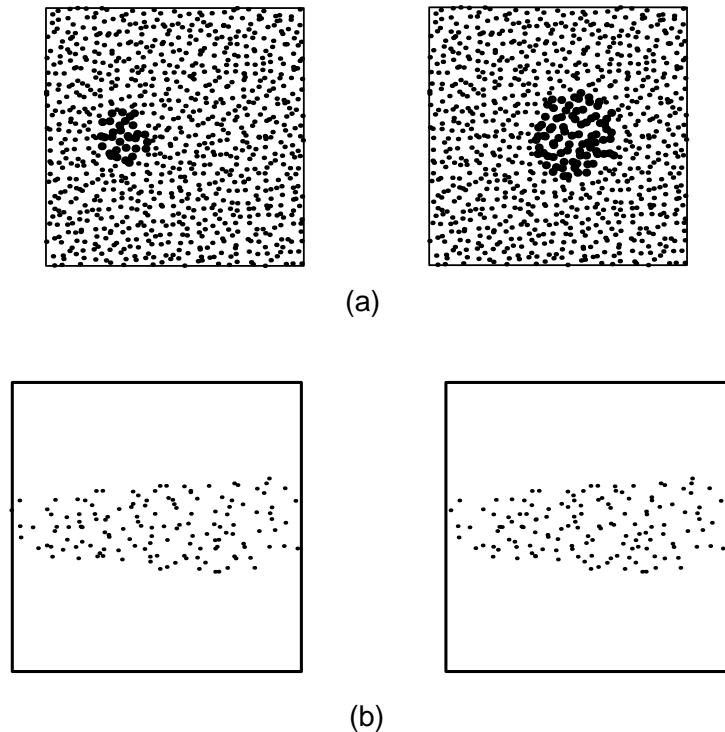


Figure 8. The border-surface algorithm applied to a growing disk. (a) First and last frames of a color-from-motion display depicting a translating and growing disk. (b) A stereo view of the border-surface points computed by the algorithm. The main axis of the 3D cylinder represents the passage of time.

As noted above displays of color from motion in which the color of dots is assigned probabilistically can be created (Cicerone & Hoffman, 1997). Each dot inside is, say, green; while each dot outside has a higher probability of being red, but some probability of being green. Over a range of probabilities in such displays, viewers can still see a subjective contour despite a high degree of color inhomogeneity. This suggests that, to handle this color inhomogeneity, there may be a process prior to the point-aperture problem in which the visual system uses spatial and/or temporal windows to compute statistics to determine “inside” versus “outside” decisions for each dot. For example, green dots outside the filter may be consistent with a background of multicolored dots, against which a green object or filter must be detected. Once this decision is made, the results can then be fed into the point-aperture algorithms as presented here.

Our approach differs from the related work of Basri, Grove, and Jacobs (1998) and of Lindenbaum and Bruckstein (1988): They assume that portions of the bounding contour of the object are visible and can be obtained in single static images. As we noted in the introduction, we assume that no portion of the bounding contour is visible in any static image, and that the bounding contour must be constructed entirely from properties of the sequence of images.

It is of some interest to find neural correlates of the illusory boundaries perceived in displays of color from motion. Studies with standard illusory boundaries are encouraging. Using single cell recordings, von der Heydt, Peterhans, and Baumgartner (1984) found that almost half of the neurons

in area V2 of macaque visual cortex can respond to the presence of moving illusory contours. They have subsequently studied this effect in great detail (Peterhans and von der Heydt 1989; 1991; Peterhans, von der Heydt, and Baumgartner 1986; von der Heydt and Peterhans 1989a; 1989b). All these studies used illusory contours generated by abutting line gratings or by two parallel bars with aligned rectangular notches. Using similar stimuli, Redies, Crook, and Creutzfeld (1986) found that some complex cells in visual areas 17 and 18 of the cat also respond to illusory contours, although Gregory (1987) failed to replicate this finding. And Grosz, Shapley, and Hawken (1993) found complex and simple cells in V1 of macaques that respond to illusory contours. In each of these studies the experimenters moved real contours to produce the effect of illusory contours. It would be of interest to see if cells in V1 or V2 can respond to illusory contours formed without any motion of any “real” contours, i.e., by displays of color from motion. If so, this would challenge most current neural network models of illusory contours, which rely on edges and their orientations to construct the illusory contours (Peterhans et al. 1986; Finkel and Edelman 1989; Finkel and Sajda 1992; 1994; Sajda and Finkel 1992a; 1992b; 1995; Kellman and Shipley 1991; Grossberg and Mingolla 1985a; 1985b; 1987a; 1987b; Grossberg 1994). Displays of color from motion demonstrate that human vision does not require real motion, oriented edges, or discontinuities to see illusory contours. Perhaps the same is true of some of its neurons.

An interesting open question is the precise form of the functional to be optimized in the construction of such curves and surfaces.

ACKNOWLEDGEMENTS

For helpful discussions we thank Andrea van Doorn, Heiko Hecht, Jan Koenderink, Manish Singh, Lothar Spillmann, and Dejan Todorović. This work was supported by a grant from the Zentrum für interdisziplinäre Forschung der Universität Bielefeld, Germany (D.D.H.) and by PHS-NIH/NEI Grant EY71132 (C.M.C.).

REFERENCES

- Adelson, E.A. & Movshon, J.A. (1982). Phenomenal coherence of moving visual patterns. *Nature*, *300*, 523–525.
- Andersen, G.J., & Braunstein, M.L. (1983). Dynamic occlusion in the perception of rotation in depth. *Perception & Psychophysics*, *34*, 356–362.
- Andersen, G.J., & Cortese, J.M. (1989). 2-D contour perception resulting from kinetic occlusion. *Perception & Psychophysics*, *46*, 49–55.
- Blake, A. (1989). Comparison of the efficiency of deterministic and stochastic algorithms for visual reconstruction. *IEEE Transactions on Pattern Analysis & Machine Intelligence*, *11*, 2–12.
- Bruno, N. and Bertamini, M. (1990). Identifying contours from occlusion events. *Perception & Psychophysics*, *48*, 331–342.

- Cicerone, C.M. & Hoffman, D.D. 1991. Dynamic neon colors: Perceptual evidence for parallel visual pathways. *University of California, Irvine, Mathematical Behavior Sciences Memo* 91–22.
- Cicerone, C.M., & Hoffman, D.D. (1997). Color from motion: dioptic activation and a possible role in breaking camouflage. *Perception*, 26, 1367–1380.
- Cicerone, C.M., Hoffman, D.D., Gowdy, P.D., and Kim, J.S. (1995). The perception of color from motion. *Perception & Psychophysics*, 57, 761–777.
- Cortese, J.M., & Andersen, G.J. (1991). Recovery of 3-D shape from deforming contours. *Perception & Psychophysics*, 49, 315–327.
- Cunningham, D.W., Shipley, T.W., & Kellman, P.J. (1998). Interactions between spatial and spatiotemporal information in spatiotemporal boundary formation. *Perception & Psychophysics*, 60, 839–851.
- Finkel, L.H., & Edelman, G.M. (1989). Integration of distributed cortical systems by reentry: A computer simulation of interactive functionally segregated visual areas. *Journal of Neuroscience*, 9, 3188–3208.
- Finkel, L.H., & Sajda, P. (1992). Object discrimination based on depth-from-occlusion. *Neural Computation*, 4, 901–921.
- Finkel, L.H., & Sajda, P. (1994). Constructing visual perception. *American Scientist*, 82, 224–237.
- Foley, J., Van Dam, A. (1982). *Fundamentals of interactive computer graphics*. Reading, MA: Addison-Wesley.
- Giblin, P.J., Pollick, F.E., and Rycroft, J.E. (1994). Recovery of an unknown axis of rotation from the profiles of a rotating surface. *Journal of the Optical Society of America A*, 11, 1976–1984.
- Gibson, J.J. (1979). *The Ecological Approach to Visual Perception*. Boston, MA: Houghton Mifflin.
- Gibson, J.J., Kaplan, G.A., Reynolds, H.N. Jr., and Wheeler, K. (1969). The change from visible to invisible: A study of optical transitions. *Perception & Psychophysics*, 5, 113–116.
- Grimson, W.E.L. (1981). *From Images to Surfaces: A Computational Study of the Human Early Visual System*. Cambridge, MA: MIT Press.
- Gregory, R.L. (1987). Illusory contours and occluding surfaces. In S. Petry & G.E. Meyer (Eds.), *The perception of illusory contours* (pp 81–89). New York: Springer-Verlag.
- Grosz, D.H., Shapley, R.M., and Hawken, M.J. (1993). Macaque V1 neurons can signal “illusory” contours” *Nature*, 365, 550–552.
- Grossberg, S. (1994). 3-D vision and figure-ground separation by visual cortex. *Perception & Psychophysics*, 55, 48–121.
- Grossberg, S., & Mingolla, E. (1985a). Neural dynamics of form perception: Boundary completion, illusory figures, and neon color spreading. *Psychological Review*, 92, 173–211.

- Grossberg, S., & Mingolla, E. (1985b). Neural dynamics of perceptual grouping: Tethers, boundaries, and emergent segmentations. *Perception & Psychophysics*, *38*, 141–171.
- Grossberg, S., & Mingolla, E. (1987a). Neural dynamics of surface perception: Boundary webs, illuminants, and shape from shading. *Computer Vision, Graphics, & Image Processing*, *37*, 116–165.
- Grossberg, S., & Mingolla, E. (1987b). The role of illusory contours in visual segmentation. In S. Petry & G.E. Meyer (Eds.), *The perception of illusory contours* (pp 116–125). New York: Springer-Verlag.
- Heitger, F., & von der Heydt, R. (1993). A computational model of neural contour processing: Figure-ground segregation and illusory contours. In *IEEE 4th International Conference on Computer Vision* (pp 32–40). Los Alamitos, CA: IEEE Computer Society Press.
- Kellman, P.J., & Cohen, M.H. (1984). Kinetic subjective contours. *Perception & Psychophysics*, *35*, 237–244.
- Kellman, P.J., & Shipley, T.F. (1991). A theory of visual interpolation in object perception. *Cognitive Psychology*, *23*, 141–221.
- Koenderink, J. (1995). Personal communication, November 23.
- Kaplan, G.A. (1969). Kinetic disruption of optical texture: The perception of depth at an edge. *Perception & Psychophysics*, *6*, 193–198.
- Liebmann, S. (1927). Über das Verhalten farbiger Formen bei Helligkeitsgleichheit von Figure und Grund. *Psychologische Forschung*, *9*, 300–353.
- Marr, D., & Ullman, S. (1981). Directional selectivity and its use in early visual processing. *Proceedings of the Royal Society of London Series B*, *211*, 151–180.
- Metzger, W. (1953). *Gesetze des Sehens*, 2nd ed. (Frankfurt: Waldemar Kramer).
- Miyahara, E., & Cicerone, C.M. (1997). Color from motion: separate contributions of chromaticity and luminance. *Perception*, *26*, 1381-1396.
- Musatti, C.L. (1975). Stereokinetic phenomena and their interpretation. In G B Flores D'Arcais (Ed.), *Studies in Perception: Festschrift for Fabio Metelli*. Milan: Martello-Giunti.
- Nakayama, K., & Silverman, G.H. (1988). The aperture problem – I. Perception of nonrigidity and motion direction in translating sinusoidal lines. *Vision Research*, *28*, 739–746.
- Nakayama, K., & Silverman, G.H. (1988). The aperture problem – II. Spatial integration of velocity information along contours. *Vision Research*, *28*, 747–753.
- Palmer, E., Kellman, P.J., & Shipley, T.F. (1997). Spatiotemporal relatability in dynamic object completion. *Investigative Ophthalmology & Visual Science*, *38*, 256.
- Peterhans, E., & von der Heydt, R. (1989). Mechanisms of contour perception in monkey visual cortex: II. Contours bridging gaps. *Journal of Neuroscience*, *9*, 1749–1763.
- Peterhans, E., & von der Heydt, R. (1991). Elements of form perception in monkey prestriate cortex.

- In A. Gorea, Y. Fregnac, Z. Kapoula, & J. Findlay (Eds.), *Representations of vision—Trends and tacit assumptions in vision research* (pp 1–12). Cambridge, UK: Cambridge University Press.
- Peterhans, E., von der Heydt, R., and Baumgartner, G. (1986). Neuronal responses to illusory contour stimuli reveal stages of visual cortical processing. In J.D. Pettigrew, K.J. Sanderson, & W.R. Levick (Eds.), *Visual Neuroscience* (pp 343–351). Cambridge, UK: Cambridge University Press.
- Pollick, F.E. (1994). Perceiving shape from profiles. *Perception & Psychophysics*, 55, 152–161.
- Redies, C., Crook, J.M., and Creutzfeldt, O.D. (1986). Neuronal responses to borders with and without luminance gradients in cat visual cortex and dorsal lateral geniculate nucleus. *Experimental Brain Research*, 61, 469–481.
- Rock, I., & Halper, F. (1969). Form perception without a retinal image. *American Journal of Psychology*, 82, 425–440.
- Sajda, P., & Finkel, L.J. (1992a). Cortical mechanisms for surface segmentation. In F. Eeckman & J. Bower (Eds.), *Computation and neural systems 1992* (p 10). Boston, MA: Kluwer.
- Sajda, P., & Finkel, L.J. (1992b). Simulating biological vision with hybrid neural networks. *Simulation*, 59, 47–55.
- Sajda, P., & Finkel, L.J. (1995). Intermediate-level visual representations and the construction of surface perception. *Journal of Cognitive Neuroscience*, 7, 267–291.
- Scott, T.R., & Noland, J.H. (1965). Some stimulus dimensions of rotating spirals. *Psychological Review*, 72, 344–357.
- Shipley, T.F., & Kellman, P.J. (1993). Optical tearing in spatiotemporal boundary formation: When do local element motions produce boundaries, form, and global motion? *Spatial Vision*, 7, 323–339.
- Shipley, T.F., & Kellman, P.J. (1994). Spatiotemporal boundary formation: Boundary, form, and motion perception from transformations of surface elements. *Journal of Experimental Psychology: General*, 123, 3–20.
- Shipley, T.F., & Kellman, P.J. (1997). Spatiotemporal boundary formation: The role of local motion signals in boundary perception. *Vision Research*, 37, 1281–1293.
- Stumpf, P. (1911). Über die Abhängigkeit der visuellen Bewegungsempfindung und ihres negativen Nachbildes von den Reizvorgängen auf der Netzhaut. *Zeitschrift für Psychologie*, 59, 321–330.
- Szeliski, R. (1990). Fast surface interpolation using hierarchical basis functions. *IEEE Transactions on Pattern Analysis & Machine Intelligence*, 12, 513–528.
- Todd, J.T., & Norman, J.F. (1991). The visual perception of smoothly curved surfaces from minimal apparent motion sequences. *Perception & Psychophysics*, 50, 509–523.

- Todorović, D. (1993). Analysis of two- and three-dimensional rigid and nonrigid motions in the stereokinetic effect. *Journal of the Optical Society of America A*, *10*, 804–826.
- von der Heydt, R., Peterhans E., and Baumgartner G. (1984). Illusory contours and cortical neuron responses. *Science*, *224*, 1260–1262.
- von der Heydt, R., & Peterhans, E. (1989a). Cortical contour mechanisms and geometrical illusions. In D.M. Lam & C.D. Gilbert (Eds.), *Neural mechanisms of visual perception* (pp 157–170). The Woodlands, Texas: Portfolio Publishing.
- von der Heydt, R., & Peterhans, E. (1989b). Mechanisms of contour perception in monkey visual cortex: I. Lines of pattern discontinuity. *Journal of Neuroscience*, *9*, 1731–1748.
- Wallach, H. (1935). Über visuell wahrgenommene Bewegungsrichtung. *Psychologische Forschung*, *20*, 325–380.
- Wallach, H. (1976). The direction of motion of straight lines. In H. Wallach (Ed.), *On Perception*. New York: Quadrangle.
- Waxman, A.M., & Wohn, K. (1988). Image flow theory: a framework for 3-D inference from time-varying imagery. In C.M. Brown (Ed.), *Advances in Computer Vision: Vol. 1* Hillsdale, NJ: Erlbaum.
- Weiss, I. (1990). Shape reconstruction on a varying mesh. *IEEE Transactions on Pattern Analysis & Machine Intelligence*, *12*, 345–362.
- Yonas, A., & Granrud, C.E. (1985). The development of sensitivity to kinetic, binocular, and pictorial depth information in human infants. In D.J. Ingle, M. Jeannerod, and D.N. Lee (Eds.), *Brain Mechanisms and Spatial Vision* (pp 113–145). Dordrecht, the Netherlands: Martinus Nijhoff.
- Yuille, A.L., & Grzywacz, N.M. (1988). A computational theory for the perception of coherent visual motion. *Nature*, *333*, 71–74.